Electronic Supplementary Material (ESI) for Nanoscale.

Size and Temperature Dependent Shapes of Copper Nanocrystals using Replica-Exchange Molecular Dynamics Simulations

Huaizhong Zhang, [†,1] Mohd Ahmed Khan, [†,1] Tianyu Yan, [†,1] and Kristen A. Fichthorn*[†‡]

†*Department of Chemical Engineering, The Pennsylvania State University, University Park, Pennsylvania 16802, USA*

‡*Department of Physics, The Pennsylvania State University, University Park, Pennsylvania 16802, USA*

E-mail: fichthorn@psu.edu

[1]Equal contributions by both authors.

Details of PTMD Simulations

The general workflow for our study is as follows: We begin by constructing a nanocrystal consisting of N atoms. To do this we create magic-sized Ih, Dh, and single-crystal structures and we either add or remove atoms at the surface to achieve the desired size. After constructing a nanocrystal, we place it in a cubic and periodic simulation box with dimensions of 100Å × 100Å × 100Å and subject it to a five ns equilibration in the canonical *(NVT)* ensemble at 300 K using MD. Next, we generate M replicas of the equilibrium nanocrystal to serve as initial configurations for a PTMD simulation. We also utilize nanocrystals generated in prior PTMD runs as initial shapes for subsequent PTMD runs.

In the PTMD simulations, each of the M replicas is assigned an initial temperature, ranging from the lowest T_1 to the highest T_M. The lowest temperature T_1 was set to 300 K, and the highest temperature T_M was 900 K and 940 K for smaller and larger nanocrystals, respectively, as discussed below. The highest temperature was chosen to be greater than the melting temperature of these nanocrystals. Parallel, canonical MD simulations were performed to simulate each of the M temperatures/replicas. Swaps between replicas were attempted every two ps, with a probability p given by

$$p = min\left(1, exp\left[\left(E_i - E_j\right)\left(\frac{1}{kT_i} - \frac{1}{kT_j}\right)\right]\right) \quad , \qquad (S1)$$

where E_i and E_j are the potential energies of replicas i and j respectively, T_i and T_j are the temperatures of replica i and j, respectively, and k is the Boltzmann constant.

Each PTMD simulation was run for a total simulation time ranging from 150 to 180 ns, depending on the nanocrystal size. After the temperature-swapping stage was complete, *NVT*

simulations were performed on each replica for an additional five ns to ensure equilibration of the nanocrystals obtained from PTMD. Each replica was controlled at the target temperature of the last PTMD swap during the final equilibration period. Throughout both the PTMD and *NVT* equilibration phases (prior to and following PTMD), the equations of motion were integrated using the velocity-Verlet algorithm with a time step of 1.0 fs. The *NVT* ensemble was maintained using the Nosé-Hoover thermostat.

At least 12 PTMD simulations were run to sample nanocrystal configurations. As we will elaborate below, we characterized the nanocrystal shape at each temperature in each PTMD run. The final distribution of nanocrystal shapes is not influenced by the initial shape, indicating that the shape distributions have converged.

Adequate temperature spacing between the PTMD replicas is necessary to achieve convergence of the nanocrystal shape distributions, especially for the larger nanocrystals. **Figure S1** illustrates this aspect. **Figure S1(a)** shows the average potential energy of each replica as a function of its corresponding average temperature during the final five ns of *NVT* equilibration for Cu_{110}. We observe a smooth increase of the potential energy with increasing temperature, with an inflection point at the melting temperature. The energy spacing between replicas with neighboring temperatures is such that replica exchange, governed by Equation (S1), occurs readily. We observe similar potential-energy profiles for nanocrystals containing between 100 and 121 atoms. For this size range, we use 31 replicas with temperatures ranging from 300 K to 900 K and a 20 K temperature spacing between replicas.

Figure S1(b) shows a potential-energy curve for Cu_{130}, where we see a discontinuous, first-order jump in the potential energy around 750 K. We cannot have efficient replica exchange across the melting range with such a large jump in potential energy, so more replicas need to be added

around the melting temperature. For a nanocrystal of 122 atoms, we used 32 replicas with an extra replica in the center of the melting range. For nanocrystals containing 130 to 190 atoms, 52 replicas have been used from 300 K to 940 K, such that more replicas have been added around the melting temperature (spaced at 1 K around the melting temperature and 20 K away from melting). Similarly, 72 replicas have been used for a nanocrystal with 200 atoms from 300 K to 940 K (spaced at 0.5 K around the melting temperature and 20 K around rest). By employing this approach, it is possible to attain convergence in simulations involving larger nanocrystals. After the REMD simulations and the final *NVT* equilibration, we minimized the energy of each nanocrystal.

Details of DFT Calculations

We employed DFT to reoptimize the structures of five different 200-atom Cu nanocrystals (FCC, SCSF, Dh, Ih and Dh-Ih) obtained from our PTMD simulations in vacuum. For these DFT calculations, we used VASP with the Projector Augmented Wave method.[1-4] A plane wave energy cutoff of 400 eV was applied, along with the Perdew-Burke-Ernzerhof parameterization of the generalized gradient approximation exchange-correlation functional.[5] The energy convergence criterion was set to 10^{-6} eV. The particles were placed in a cubic box with dimensions of (30 × 30 × 30) Å, allowing effective sampling of the Brillouin zone using the Γ point. The optimization of atomic positions continued until the forces converged to values of less than 0.01 eV/Å. For effective comparison of the nanocrystal energies between the EAM and DFT values, we also optimized the EAM nanocrystals with a force tolerance of 0.01 eV/Å. This force tolerance is higher (less precise) than the one used for energy minimizations following our PTMD simulations.

Vibrational Entropy Studies

Three distinct shapes (Dh, Ih and Dh-Ih, as shown in **Figure S6**) of Cu_{200} nanocrystals were re-optimized by DFT to determine their vibrational frequencies. The finite-difference method with DFT was employed for these calculations, utilizing VASP. Phonopy, an open-source package for phonon calculations, was also used.[6, 7] We used Phonopy to generate 1200 images for each shape. Each image represented a single atom displacement from its equilibrium structure, which we can use to conduct phonon calculations in parallel. The vibrational frequencies for each nanocrystal were determined from dynamical matrices constructed using force constants, post-processing the output from the phonon calculations.

We calculated the vibrational partition function (q_{vib}) and vibrational entropy (S_{vib}) from vibrational frequencies within the temperature range of 300 K to 750 K. The vibrational partition function (q_v) is obtained using the harmonic oscillator approximation, as shown in Equation (S2), where v_b is the frequency of vibrational mode b – for N atoms, we have $3N$-6 non-zero vibrational frequencies. In the case of large nanocrystals, many vibrational modes exhibit small frequencies. To prevent an overestimation of q_{vib} due to the anharmonic nature of vibrations with small frequencies, we set a cut-off frequency of 2.4 THz and we raised any frequency below the cut-off value to the cut-off. This has been done in other studies in the literature.[8, 9]

$$q_v = \prod_b \frac{e^{-\frac{\hbar v_b}{2kT}}}{1 - e^{-\frac{\hbar v_b}{kT}}} \quad . \qquad (S2)$$

The vibrational entropy (S_v) was subsequently calculated using

$$S_v = kln(q_v) \quad . \qquad (S3)$$

Figures

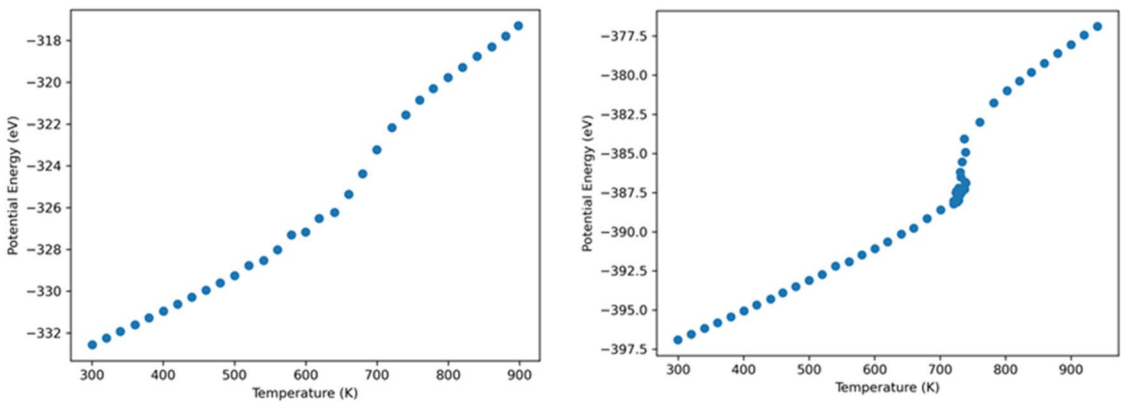

Figure S1. The average potential energy as a function of temperature during the final equilibration period from PTMD simulations of Cu nanocrystals containing (a) 110 atoms and (b) 130 atoms.

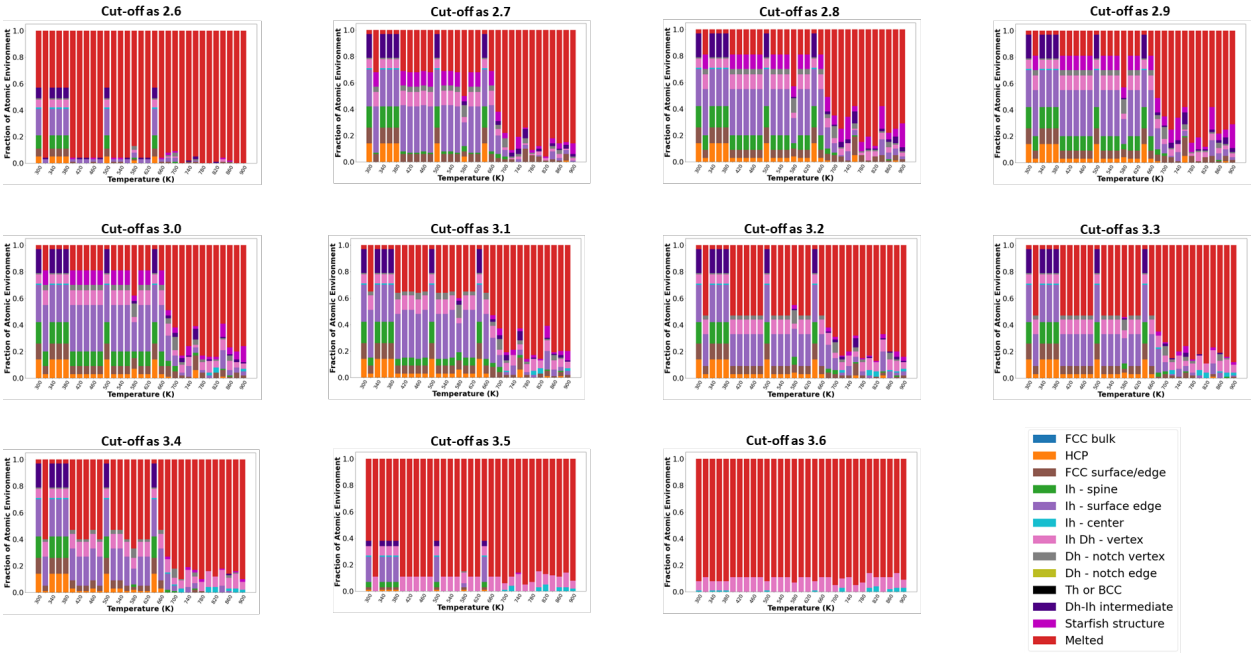

Figure S2. Effect on CNA environment of changing the cut-off value (in Å) for Cu_{100}.

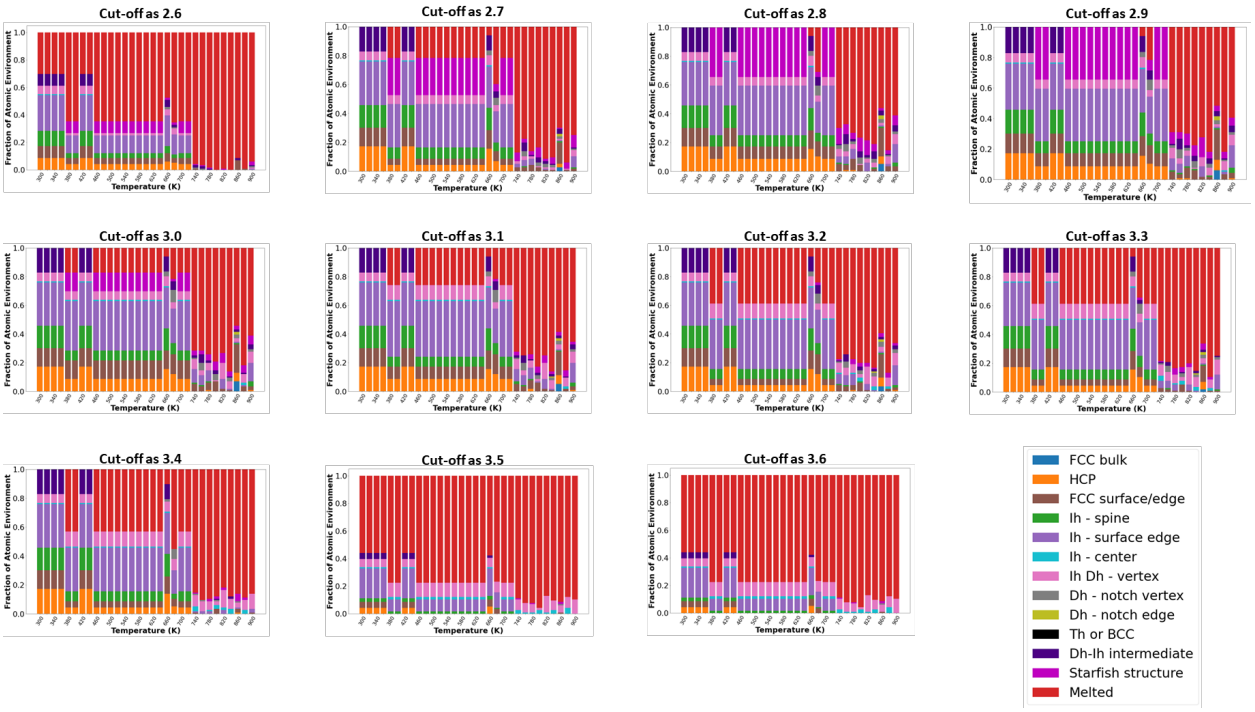

Figure S3. Effect on CNA environment of changing the cut-off value (in Å) for Cu_{116}.

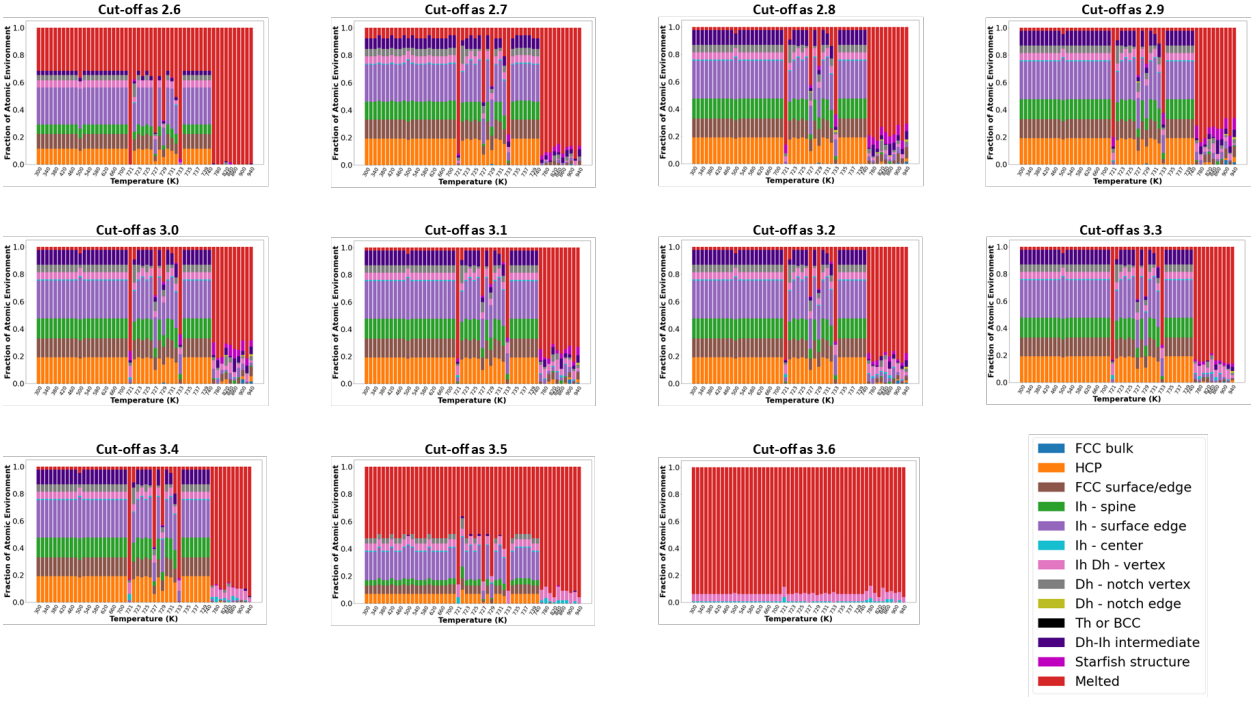

Figure S4. Effect on CNA environment of changing the cut-off value (in Å) Cu_{130}.

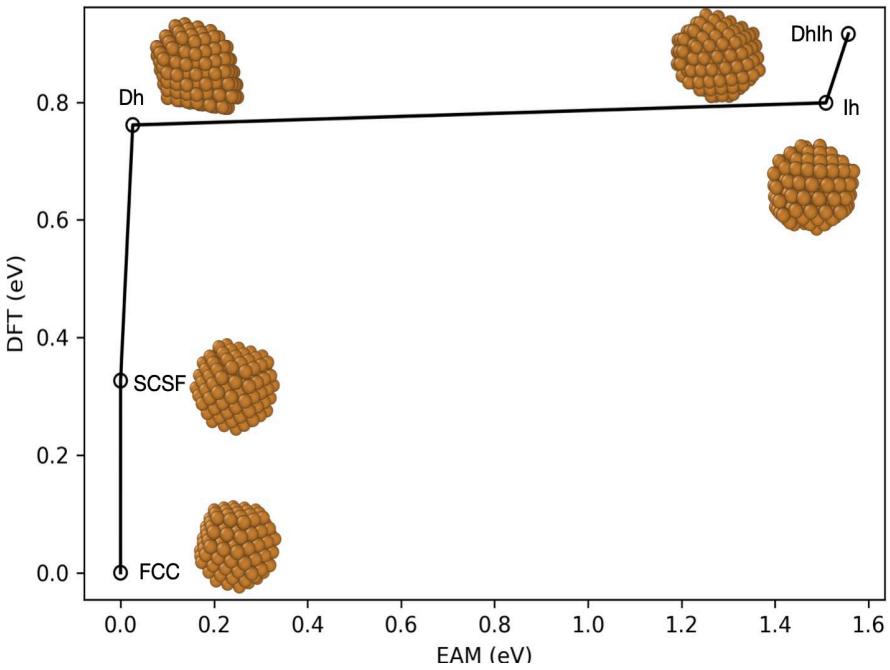

Figure S5. Comparison of the EAM and DFT energies of the most probable shape (with respect to the shape with minimum energy) in each of the five categories: FCC, SCSF, Dh, Ih and Dh-Ih for nanocrystals containing 200 atoms. The insets show the most probable shapes.

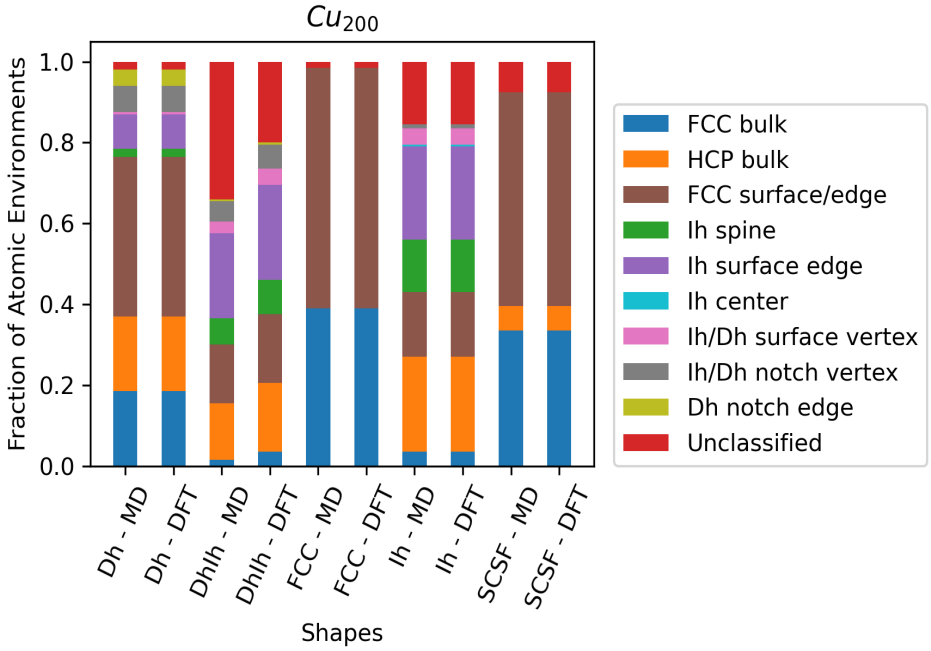

Figure S6. Distribution of CNA environments in Cu_{200} nanocrystals with the most probable shape in each of the five categories: Dh, DhIh, FCC, Ih and SCSF from the EAM potential (MD) and from EAM nanocrystals re-optimized using DFT.

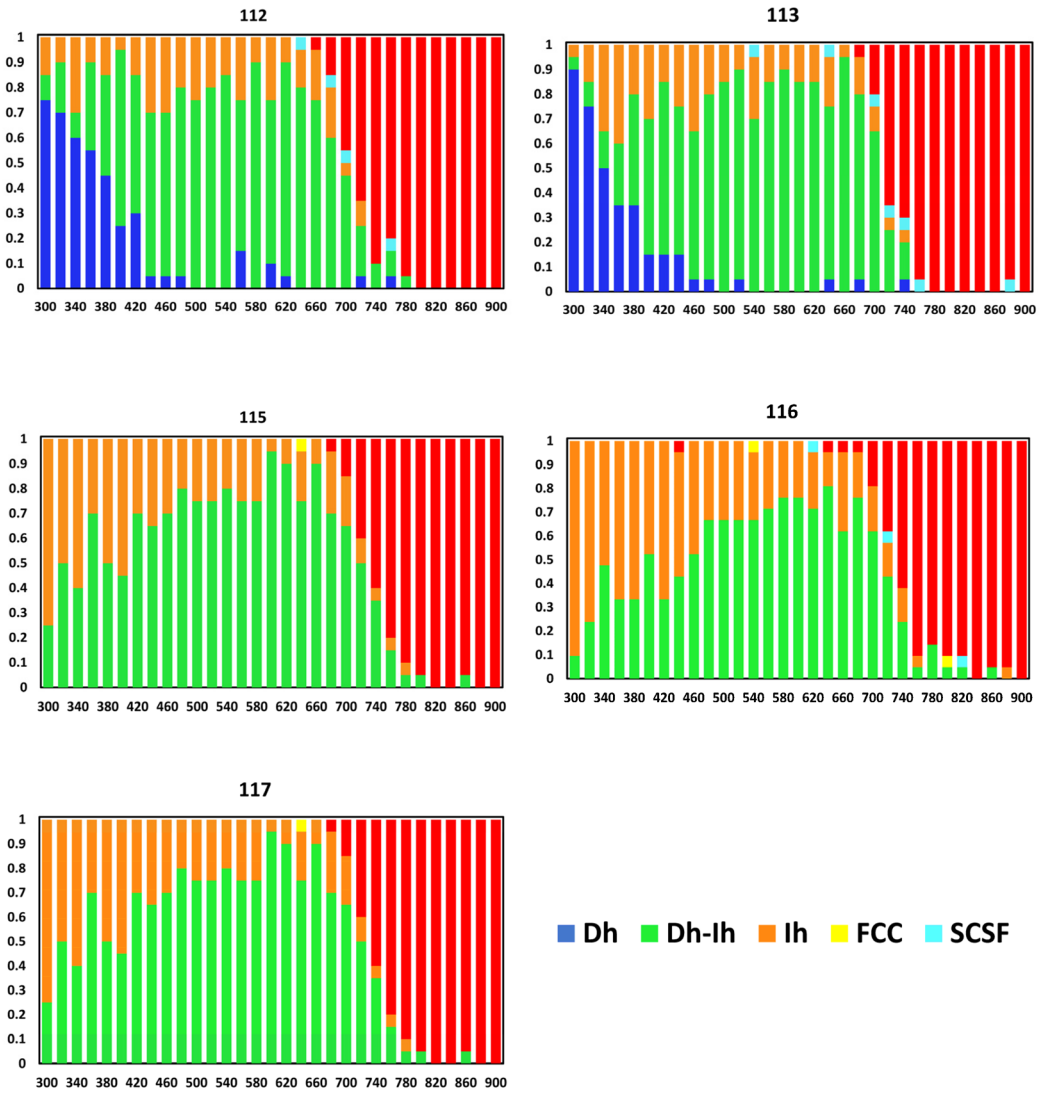

Figure S7. Nanocrystal shape distributions (fractions) as a function of temperature (K) for select sizes.

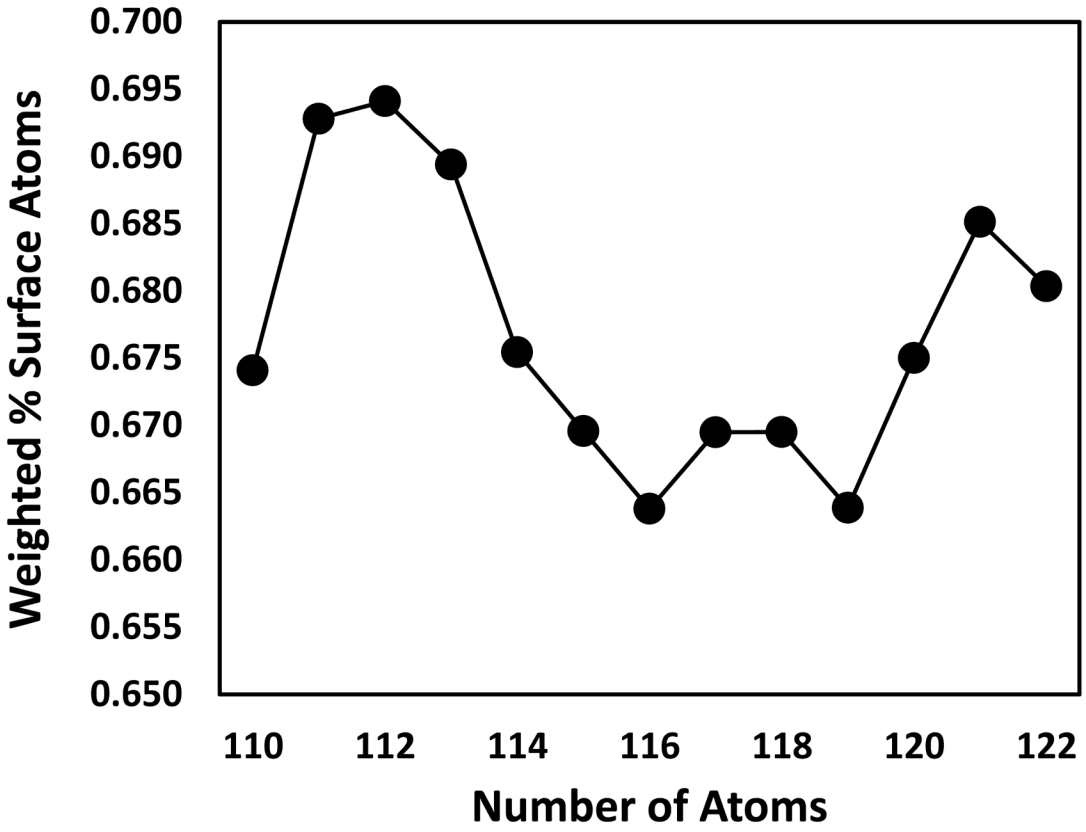

Figure S8. Percentage of surface atoms, weighted by shape percent at 300 K, as a function of nanocrystal size. Surface atoms are defined as atoms with a coordination number (C_N in **Table 1**) of less than 11.

References

1. G. Kresse and J. Furthmüller, *Phys. Rev. B*, 1996, **54**, 11169-11186.
2. G. Kresse and J. Hafner, *Phys. Rev. B*, 1994, **49**, 14251-14269.
3. G. Kresse and J. Hafner, *Phys. Rev. B*, 1993, **47**, 558-561.
4. P. E. Blochl, *Phys. Rev. B*, 1994, **50**, 17953-17979.
5. J. P. Perdew, K. Burke and M. Ernzerhof, *Phys. Rev. Lett.*, 1996, **77**, 3865-3868.
6. A. Togo, *J. Phys. Soc. Jpn.*, 2023, **92**.
7. A. Togo, L. Chaput, T. Tadano and I. Tanaka, *J. Phys. Condens. Matter*, 2023, **35**, 353001.
8. Z. H. Li, A. W. Jasper and D. G. Truhlar, *J. Am. Chem. Soc.*, 2007, **129**, 14899-14910.
9. S. Jindal and S. S. Bulusu, *J. Chem. Phys.*, 2020, **152**, 154302.